Published in final edited form as:
J Mol Biol. 2007 October 19; 373(2): 315–327.

Single MHC Mutation Eliminates Enthalpy Associated with T Cell Receptor Binding

Peter J. Miller[1], **Yael Pazy**[2], **Brian Conti**[1], **David Riddle**[2], **Ettore Appella**[3], and **Edward J. Collins**[1,2,4]

1*Department of Biochemistry and Biophysics, The University of North Carolina at Chapel Hill, Chapel Hill, NC, 27599, USA*

2*Department of Microbiology and Immunology, The University of North Carolina at Chapel Hill, Chapel Hill, NC, 27599, USA*

3*Laboratory of Cell Biology, National Cancer Institute, National Institutes of Health, Bethesda, MD 20892, USA*

SUMMARY

The keystone of the adaptive immune response is T cell receptor (TCR) recognition of peptide presented by Major Histocompatibility Complex (pMHC) molecules. The co-crystal structure of AHIII TCR bound to the MHC, HLA-A2, showed a large interface with an atypical binding orientation. MHC mutations in the interface of the proteins were tested for changes in TCR recognition. From the range of responses observed, three representative HLA-A2 mutants, T163A, W167A, and K66A, was selected for further study. Binding constants and co-crystal structures of the AHIII TCR and the three mutants were determined. K66 in HLA-A2 makes contacts with both peptide and TCR and previously has been identified as a critical residue for recognition by numerous TCR. The K66A mutation resulted in the lowest AHIII T cell response and the lowest binding affinity, which suggests T cell response may correlate with affinity. Importantly, the K66A mutation does not affect the conformation of the peptide. The change in affinity appears to be due to a loss in hydrogen bonds in the interface as a result of a conformational change in the TCR complementarity-determining region 3 (CDR3) loop. Isothermal titration calorimetry confirmed the loss of hydrogen bonding by a large loss in enthalpy. Our findings are inconsistent with the notion that the CDR1 and CDR2 loops of the TCR are responsible for MHC restriction, while the CDR3 loops interact solely with the peptide. Instead, we present here a MHC mutation that does not change the conformation of the peptide, yet results in an altered conformation of a CDR3.

Keywords

MHC; TCR; Binding; Structure; Cytolysis

INTRODUCTION

T cells are an integral part of the adaptive immune system's ability to recognize virtually any pathogen that might attack the host. A critical step required for T cell activation is the recognition of peptides derived from these pathogens when presented by the Major

[4]Corresponding author: edward_collins@med.unc.edu

Histocompatibility Complex protein (MHC). Recognition of foreign peptide bound to MHC is achieved through the clonotypic T cell receptor (TCR). Upon TCR recognition of a peptide bound to MHC (pMHC) sets of T cells either kill the cell presenting the foreign peptide (cytotoxic T cells) or produce cytokines to "help" B cells and other T cells (helper T cells). The pathogens are subsequently eliminated from the host by a combination of killing infected cells to remove reservoirs of replicating pathogen, and antibody-mediated neutralization of the pathogen outside of the cell. Although TCR binding to pMHC is paramount for T cell activation, there are still many unanswered questions regarding how TCR-pMHC interactions dictate T cell response.

Recognition of pMHC by the TCR heterodimer is accomplished using the three complementarity determining region (CDR) loops from each chain. The CDR1 and CDR2 loops are germ-line encoded within the variable gene segment of each TCRα and TCRβ chain. The CDR3 loop of each chain is unique and arises through V(D)J recombination [1; 2]. While recognition of the pMHC is carried out using all the CDR loops of each chain, generally the CDR3 makes more contacts with the bound peptide than CDR1 and CDR2 [3].

Engagement of TCR with pMHC may result in a variety of reactions from the T cell, and the mechanisms that generate these different responses are not understood [3]. The structures of TCR bound to partial agonist or antagonist pMHC complexes do not show changes in the TCR domains [4; 5] that would suggest a way for the TCR to propagate a qualitatively different signal to the T cell through the plasma membrane. It is generally accepted that there is great plasticity in the interaction between TCR and pMHC. However, as seen in a variety of TCR-pMHC co-crystal structures the degree and location of this plasticity is not generalizable. For example, the co-crystal structures of 2C-dEV8/K^b [6], 2C-SIYR/K^b [4], and KB5-C20-pKB1/K^b [7] when compared to crystal structures of those TCRs alone show great flexibility in the CDR3 loops of the TCR. The LC13 [8] and BM3.3 [9] TCRs undergo changes in not just their CDR3s, but also their CDR1 and CDR2 loops. Conversely, the A6-Tax/A2 [10] and ELS4-EPLP/B*3501 [11] co-crystal structures exhibit conformational changes in the peptides upon TCR-pMHC binding. Finally, the crystal structures of the 1G4 TCR alone and complexed with its pMHC ligands show no significant changes in either the TCR or the pMHC [12].

Similarly, there appear to be no general thermodynamic rules that describe TCR binding to pMHC. Although surface plasmon resonance (SPR) has been used for more than a decade to examine binding of TCR to pMHC, it measures kinetic constants between TCR and pMHC and binding via Scatchard Analysis or mathematically using the kinetic constants. Isothermal titration calorimetry (ITC) provides a direct measure of ΔH and is hence considered a more reliable determination of thermodynamic parameters. ITC has been rarely utilized for TCR-pMHC studies because of the much larger amounts of protein required for the studies. Early experiments suggested that TCR-pMHC interactions seem to be governed by large enthalpically favorable and entropically unfavorable thermodynamics [13; 14; 15; 16]. However, more recent thermodynamic data of L13-FLR/B8 [17], A6-Tax/A2 [18], and 2C-QL9/L^d [19] all show entropically favorable associations.

The human MHC, HLA-A2, is the most frequent MHC found in Caucasians and African Americans [20]. A large panel of A2 mutants were created and tested against a panel of T cells. Most interesting from that study, the K66A mutant was found to adversely affect recognition of 98% of the T cells examined [21]. K66 has been shown to be a critical residue in TCR recognition of A2, regardless of the peptide presented [21; 22; 23; 24], resulting in K66 to be labeled a potential "hot spot" for TCR recognition of A2. Importantly, even though K66 interacts with the peptide, the structure of Tax/A2(K66A) shows that the K66A mutation does not alter the structure of A2 or the conformation of the Tax peptide [24]. However, the effect of the K66A mutation on the cognate TCR has never been determined structurally.

AHIII12.2 (AHIII) is a murine T cell clone that recognizes human HLA-A2.1 [25] when peptide 1049 (ALWGFFPVL) is presented [26]. Reactivity towards p1049/A2 does not require binding of the TCR co-receptor CD8, [27] which allows for the study of TCR-pMHC interactions without the additional complexity of the third protein. We have previously described the crystal structure of the AHIII TCR complexed with p1049/A2 [28]. From the AHIII-p1049/A2 co-crystal structure, we identified a number of A2 surface residues that may be responsible for binding the AHIII TCR. These residues were mutated in A2 and the changes in T cell cytolytic activity were examined as a function of the mutation. Three mutants were then selected for kinetic, thermodynamic, and structural studies. Most importantly, the K66A mutation causes substantial changes to cytotoxicity and the affinity. This change in affinity appears to be due to a large reduction in hydrogen bonding that is a result of a large conformational change in the CDR3 loop. This loss of hydrogen bonding is reflected in the almost complete loss of enthalpy in the binding reaction.

RESULTS

AHIII T Cell Reactivity

Based on the co-crystal structure of AHIII bound to p1049/A2 [28], thirteen HLA-A2 mutations were selected to probe the interface. The ability of AHIII T cells to lyse target cells expressing this panel of A2 variants was assessed by loading the target cells with radioactive chromium (^{51}Cr), incubating the T cells with the target cells for four hours and then measuring the radioactivity released to the media. Measured lysis was normalized to AHIII lysis of wild-type A2 expressing cells in each experiment. A spectrum of responses to the mutations was seen (Figure 1). Some of the mutants showed little affect on reactivity (E166A and T163A). On the other end of the spectrum the K66A mutation almost completely abolished the response. In addition to the K66 “hot spot” in A2 [21; 22; 23; 24], it has been suggested that positions 65, 69, and 155 could be critical to MHC-restriction due to the high frequency with which they are seen contacting TCRs in determined TCR-pMHC structures [3; 29; 30]. Consistent with those data, mutations at positions 65, 69, and 155 all had deleterious effects on AHIII cytotoxicity.

Three A2 variants that represent the range of T cell reactivity were chosen for further study: T163A (high), W167A (medium), and K66A (low). Mutant proteins were expressed recombinantly as inclusion bodies in *E. coli* and refolded *in vitro* with p1049 peptide. Binding to the recombinant AHIII TCR was measured using surface plasmon resonance (SPR). Binding curves for these three complexes in addition to wild-type A2 are shown in Figure 2. The mutations in the MHC cause significant changes to the affinity for AHIII TCR (Table 1) with K_d values ranging from 4.7 μM (p1049/A2(T163A)) to 31.8 μM (p1049/A2(K66A)). The kinetics were also dramatically affected. The dissociation rates (k_{off}) were both faster and slower than wild-type p1049/A2 (0.27 s^{-1}). Interestingly, even though the affinity of AHIII for p1049/A2(K66A) is significantly lower than for wild-type A2, the dissociation rate is significantly slower (Figure 2 and Table 1). Association rates (k_{on}) were generally less affected by the substitutions, except for p1049/A2(K66A) (4.7×10^3 $M^{-1}s^{-1}$), which has a much slower on-rate compared to wild-type A2 (3.1×10^4 $M^{-1}s^{-1}$).

Structural Analysis of A2 Variants

The physical manifestation of the differences found in T cell recognition and binding was examined using x-ray crystallography. The three mutants described above (A2(K66A) A2 (T163A) and A2(W167A)) were co-crystallized with AHIII TCR. The locations of the mutations in the interface between the AHIII TCR and p1049/A2 are shown in Figure 3. Based on previous work, [5] it seemed unlikely that these relatively small alterations would cause large changes in the overall structures of the TCR or pMHC, or the docking orientation of the TCR.

Therefore, we hypothesized that the substitutions resulted in local alterations in the MHC or peptide, changing hydrogen bonds or van der Waals contacts present in our previously determined AHIII-p1049/A2 structure [28]. Crystallographic data were collected from three single co-crystals comprised of AHIII TCR complexed with p1049/A2(T163A), p1049/A2 (W167A), or p1049/A2(K66A), to a resolution of 2.4 Å, 2.5 Å, and 2.88 Å, respectively. All the crystals were nearly isomorphous with AHIII-p1049/A2 [28]. Data collection and refinement statistics can be found in Table 2.

As might be expected because of the similar level of T cell activity, no gross structural changes were observed in the structure of p1049/A2(T163A) bound to AHIII TCR (Figure 4a). For all three structures superimposition was performed using the "align" feature in PyMol [31], restraining the alignment to the α-carbons of the TCR-pMHC interface (TCR Vα, Vβ; and MHC α1, α2 and peptide). The AHIII-p1049/A2(T163A) complex superimposed onto AHIII-p1049/A2 with an RMSD of 0.20 $Å^2$. Difference electron density ($Fobs_{wild\text{-}type}$ - $Fobs_{mutant}$) maps show a large negative electron density peak in the position of the mutated residue that demonstrates the quality of the data and confirms the location of the mutation (Figure 4a). One change in the TCR was observed. The side chain of serine 99 in the TCR CDR3α has rotated into the cavity where the MHC threonine side chain is found in the wild-type structure. Interestingly, the electron density maps show the location of the serine without ambiguity, but there are no contacts visible for the serine side chain. This side chain orientation is not the most preferred rotamer [32]; that preferred conformation is found in the wild-type structure. Therefore, it may be that this position is taken to reduce undesired energetic contributions to the binding such as the fixation of solvent or the production of a cavity in the interface.

In addition to its importance to this study concerning T cell reactivity, the A2(W167A) complex was also interesting because W167 forms a boundary of the peptide-binding cleft (Figure 3) and helps form the conserved pocket that binds the amino terminus of the peptide [33]. This tryptophan is highly conserved in not only HLA-A2 subtypes (96%), but across all human class I MHC molecules (88.5%) [34]. Mutating tryptophan to alanine results in the loss of a hydrogen bond between the Trp indol nitrogen to the Tyr28 hydroxyl on the TCR CDR2 (Figure 4b). Aside from the loss of the W167-Y28 hydrogen bond, the structure of AHIII bound to p1049/A2(W167A) shows no significant changes in the peptide amino terminus, the CDR2α or CDR3α of the AHIII TCR, or the MHC itself. The mutant complex alpha carbons have an RMSD of 0.27 $Å^2$ when superimposed onto the wild-type atoms. The difference electron density ($Fobs_{wild\text{-}type}$ - $Fobs_{mutant}$) map once again shows a large negative peak in the position of the mutated residue demonstrating the quality of the data and confirming the loss of the Trp side chain. Two side chains in A2 near the site of mutation do change conformation, but these differences do not alter binding to the TCR. The amino terminus of the peptide is still coordinated by hydrogen bonds to three tyrosine hydroxyl groups Tyr7, Tyr 159, and Tyr171 of the MHC, as in wild-type p1049/A2. The AHIII-p1049/A2(W167A) structure shows weak positive difference density in the location where the nitrogen of the indole ring of wild-type Trp167 would be (data not shown). This suggests that there may be a weakly associated water molecule replacing the amine, which could hydrogen bond to the hydroxyl group on Tyr28 of CDR2α.

The structure of AHIII bound to p1049/A2(K66A) is critical to this study because of the significantly different binding constants of A2(K66A) (Table 1). Additionally, K66 on the α1 α helix of HLA-A2 has been identified as a "hot spot" for TCR recognition of HLA-A2 in a number of studies [21; 22; 23; 24]. Structures of A6-Tax/A2 [10; 35] and AHIII-p1049/A2 [28] also show that K66 is rare in that it makes critical contacts with both the TCR and the peptide. K66A mutants have increased peptide dissociation rates; yet this is not likely to be responsible for the decrease in T cell function because T cell clones have also been identified that do not have altered recognition to the K66A mutation [21; 22]. Furthermore, the K66A mutation does not

alter the MHC structure or the conformation of the Tax peptide in Tax/A2(K66A) [24]. So, if increased peptide dissociation from A2(K66A) mutants does not influence T cell activation, and the pMHC molecular surface is not altered by the mutation, the next logical hypothesis would be that the K66A variation results in a change in the TCR that negatively affects T cell function.

The co-crystal structure of AHIII-p1049/A2(K66A) determined to 2.88 Å resolution shows an altered conformation of the CDR3α of the AHIII TCR (Figure 4c). The AHIII-p1049/A2 (K66A) structure superimposes onto AHIII bound to wild-type A2 with an RMSD of 0.37 $Å^2$. The $2F_o$-F_c electron density maps show the new conformation of the loop (Figure 4d) and this location is confirmed by omit maps. The conformational change in CDR3α is that the loop appears to fill the void left by the removal of the Lys66 side chain. The Cα atoms of the loop move, on average, 2.0 Å with Ala97 moving over 4.0 Å (Table 3). This altered conformation of the loop likely disrupts the hydrogen bonding contacts found in the native structure [28] between the CDR3α and wild-type p1049/A2 (Figure 4e). In a manner similar to the Tax/A2 (K66A) structure [24], the K66A mutation does not change MHC or peptide conformation in this AHIII-p1049/A2(K66A) structure. The CDR3 loop change also negatively affects the surface complementarity (SC). The SC value for the wild-type AHIII-p1049/A2 structure is 0.71 and drops to 0.55 for AHIII-p1049/A2(K66A).

The Tax/A2(K66A) structure showed a water molecule replacing the Lys66 side chain, mediating hydrogen bonds between Glu63 of A2 and the Tax peptide [24]. There is no electron density that would suggest a water replaces the Lys66 side chain in our AHIII-p1049/A2 (K66A) structure. It appears that the new conformation of the CDR3α loop pushes further into the peptide binding cleft along the MHC α1 α helix where the Lys66 side chain would have been, displacing any water that might have filled the void before TCR binding. The number of reflections associated with the 2.88 Å resolution data can not support the modeling of water molecules in the structure of AHIII-p1049/A2(K66A). However, there is a small volume in the $2F_o$-F_c electron density map that suggests that there may be a weakly associated water molecule that would hydrogen bond with Glu63 of A2 and Ser100 on CDR3α of AHIII (Figure 4f). The only other plausible hydrogen bond between the AHIII CDR3α to p1049/A2(K66A) is from the Ser102 nitrogen to the Gly4 oxygen of the peptide (2.88 Å) (Figure 4f). In summary, there is a large alteration in the AHIII CDR3α loop when bound to p1049/A2(K66A) as compared to the wild-type complex and this alteration appears to dramatically change the number of hydrogen bonds in the complex.

Calorimetric measurement of AHIII TCR and HLA-A2 binding

The altered hydrogen bonding pattern proposed here based on the crystal structure of AHIII-p1049/A2(K66A) suggests that there should be a large change in the enthalpy of binding. To examine this directly, the heat of binding was measured using isothermal titration calorimetry (ITC). Our data show that the wild-type complex binding has a relatively small enthalpic component (-3.9 kcal/mol) and that the binding is more entropically driven (Table 4 and Figure 5a). As predicted, this small enthalpic contribution to binding is almost completely eliminated by mutation of K66 to alanine. This change is manifest clearly during the experiments because the K66A mutation changes the reaction from exothermic to endothermic (Figure 5b). The enthalpy of binding (ΔH) goes from -3.9 kcal/mol for AHIII-p1049/A2 to almost zero (-0.6 kcal/mol) for AHIII-p1049/A2(K66A). The free energy of binding (ΔG) measured for the two complexes is in agreement with those determined for other TCR-pMHC (Table 4). The thermodynamic changes for AHIII-p1049/A2(K66A) correspond to a ΔΔG of only 1.4 kcal/mol, which highlights the tight range between activating and non-activating signals for TCR.

DISCUSSION

The initial goal of this study was to determine how structural alterations in the TCR are responsible for the spectrum of T cell cytolysis by AHIII T cells. Mutations in HLA-A2 were made and changes in cytolysis examined as a function of the mutation. Recombinant protein for three A2 variants was produced and binding constants were determined by surface plasmon resonance (SPR). Surprisingly, A2(K66A) showed very different kinetic constants as compared to the wild-type complex. Structural studies showed that most hydrogen bonds involving the CDR3α loop in the complex were lost upon mutation. Isothermal titration calorimetry (ITC) confirmed a greatly decreased enthalpy of binding associated with the conformational change of the loop.

Based on the AHIII-p1049/A2 co-crystal structure previously determined [28], A2 residues that were predicted to be involved in binding the AHIIII TCR were mutated. The AHIII T cells reacted with a full spectrum of outcomes from very low cytotoxicity to slightly improved cytotoxicity as a result of changing residues in the interface between the proteins. Residues at positions 66 [21; 22; 23; 24] and 65, 69, and 155 [3; 29; 30] have all been previously identified as critical contacts in a number of TCR-pMHC systems. Mutations at all of these four of these positions in A2 resulted in a reduction of AHIII T cell cytotoxicity of 30% to almost 100%. Clearly, these residues are critical for AHIII TCR binding. As an important control, it has been shown previously that peptide binding does not change significantly for the mutations studied except K66A (it has a faster peptide off-rate) [22]. However, this faster peptide off-rate cannot account for the changes in activity because T cells can be found that are not affected by the K66A mutation [21; 22]. This implies that significant peptide bound to MHC remains on the cell surface even with the K66A mutation. In addition, the expression levels of the various mutants studied here were confirmed to be similar by flow cytometry (data not shown). Therefore, any observed changes in reactivity, binding, or structure should be due to changes in how the complexes interact. A more thorough study of how those mutations resulted in a change of function was then initiated.

A sub-set of the MHC mutants that represent dramatically reduced to full reactivity (K66A, W167A, and T163A, respectively) were chosen to study the physical manifestation of the differences. TCR-pMHC binding studies were performed using SPR. While all mutants showed some degree of change from wild-type A2, the K66A mutation resulted in remarkably slower on and off-rates than the wild-type complex. The three mutant complexes were then co-crystallized with AHIII TCR. The structures were determined and compared to the wild-type co-crystal structure. Similar to the results seen for the altered peptide ligands for the Tax/A2 specific TCR [5], there were no gross differences in any of the structures examined. Significantly, there were no changes in domain packing of the TCR that would suggest a mode to transmit information through the domains to the interior of the cell to confer different activities, as previously suggested [14]. There is always the possibility that the domain movements are dynamic and/or weakly manifested and are overcome here by crystal packing forces that would make it impossible to view using protein crystallography. Similarly, it has been suggested that upon TCR-pMHC interaction, a conformational change in the AB loop of the TCR Cα domain is required for signaling into the cell [8]. Although the position of the AB loop for the non-liganded AHIII TCR is unknown, the loop in the AHIII TCR bound to all p1049/A2, even p1049/A2(K66A), is identical, and is the same conformation as seen in the liganded LC13 TCR [8]. Importantly, the AB loop in the AHIII structures are not involved in any crystal contacts. These data imply that the AB loop has no impact on the level of cytotoxicity seen in the AHIII system.

There are no definitive structural explanations for the “improved” AHIII T cell reactivity for the A2(T163A) mutant. With threonine being conserved in 98% of all known HLA-A2

subtypes [34], we had expected a greater impact mutating it to alanine. If anything, the rotation of the TCR CDR3α Ser99 into the cavity formed by the removal of the MHC threonine side chain would be expected to contribute negatively to the binding due to the less favorable rotamer that is chosen. There are no hydrogen bonding partners near the new position of the serine hydroxyl. There is no significant increase in the complementarity in the fit between the complexes. The complementarity of fit of AHIII to p1049/A2(T163A) is 0.72 versus 0.71 for the wild-type structure. We conclude that the most likely explanation for the slightly increased binding affinity is that there is a set of very subtle changes that increase the complementarity of fit.

The A2(W167A) mutation results in a 20% loss in lysis by the AHIII T cells. There are no significant structural changes other than the loss of the W167-Y28 hydrogen bond. Loss of the W167 indole also affects surface complementarity between AHIII-p1049/A2(W167A) (SC = 0.68) compared to AHIII-p1049/A2 (SC = 0.71). Therefore, the dramatic loss of affinity to the AHIII TCR is likely a result of the lost hydrogen bond and the concomitant loss of complementarity (ie van der Waals contacts). The fact that the absence of the indole group from the end of the peptide binding cleft in the AHIII-p1049/A2(W167A) structure did not significantly alter the conformation of the bound peptide is surprising. Tryptophan is present at position 167 in 96% of all known HLA-A2 subtypes and 88.5% conserved in all human class I MHC molecules [34]. It begs the question, why is this amino acid so highly conserved? Unfortunately, the data provided in the AHIII-p1049/A2(W167A) structure are unable to address this.

Of all the mutants tested, the K66A mutation caused the largest decrease in AHIII cytolysis. The slow on-rate seen for AHIII-p1049/A2(K66A) and significant energy barriers measured for other TCR-pMHC [36; 37] imply that there are structural changes associated with binding, and in fact, a large change was seen in the CDR3α loop of the AHIII TCR. This suggests that binding requires a conformational change in the TCR, but when exactly does this occur? Does the AHIII TCR make initial contact with p1049/A2(K66A) and then the CDR3α loop moves (induced-fit) or does p1049/A2(K66A) associate with a minority member of the population of the AHIII TCRs in solution (pre-existing equilibrium). The induced-fit or two-step model [38] has been a popular means of describing TCR-pMHC interaction. However, the validity of the two-step model has been questioned by both thermodynamic [36] and structural [8; 9; 12] data. We propose that a pre-existing equilibrium model better describes TCR-pMHC association. The idea that CDR loops exist in alternative pre-existing conformations in solution has been shown in antibody crystal structures [39]. Knowing the structural similarities between antibodies and TCR, it is easy to imagine this binding mechanism to exist for TCR and pMHC. The total number of possible conformations that the CDR loops can adopt is finite and limited by the conserved framework regions of the TCR and/or antibody structure [40; 41; 42; 43]. The residues that constitute the loop will maintain phi and psi angles that allow for the lowest potential energy. Loops in higher potential energy conformations would be found less often in the population (minority member). Therefore, the pMHC surface that allows the TCR to have the greatest number of its CDR loops in conformations with the lowest energy would provide the most stable interaction, a higher affinity, and subsequent greater activation of the T cell. The structural and thermodynamic data presented here for AHIII TCR-p1049/A2(K66A) demonstrates this relationship between energetics and activation. When the CDR3α loop is required to take a conformation with higher energy, the interactions between TCR and pMHC suffer, and T cell activation is adversely affected. As there is not currently a structure of the AHIII TCR alone, we cannot be sure where the CDR3α loop lies when it is free in solution. However, the on-rate of AHIII-p1049/A2(K66A) being an order of magnitude slower than wild-type AHII-p1049/A2 binding, suggests the loop to undergo greater change in order to bind p1049/A2(K66A) than wild-type p1049/A2. We propose the TCR conformations seen in

our AHIII-p1049/A2(K66A) complex are minor in the population, so the longer k_{on} is a reflection of the unfavorable equilibrium of the pMHC binding that minority member.

The AHIII-p1049/A2(K66A) structure also suggested most of the hydrogen bonds found between AHIII CDR3α and wild-type p1049/A2 are not present in the mutant structure. The conformational change in CDR3α potentially leaves only the Ser102 to Gly4 hydrogen bond. This suggested that the enthalpy of binding is greatly diminished. The ITC data complement the structural data, as it shows there is a significant loss in binding enthalpy. Due to the small amount of heat absorbed upon AHIII-p1049/A2(K66A) binding, the titration curve generated is not satisfactory to allow for confident analysis of the entropy in the system. However, the endothermic binding combined with the loss of enthalpy suggests that the binding of AHIII TCR to p1049/A2(K66A) is nearly entirely entropically driven. For TCR-pMHC complexes where heats of binding have been measured directly (and inferred from van't Hoff calculations), the enthalpic and entropic contributions are different for each TCR-pMHC system without any unifying thermodynamic properties. Originally it was thought that TCR-pMHC interactions were governed by enthalpically favorable and entropically unfavorable thermodynamics features [13; 14; 15]; however, AHIII-p1049/A2 joins LC13-FLR/B8 [17], A6-Tax/A2 [18], and 2C-QL9/L^d [19] as TCR-pMHC systems that rely on entropically favorable binding.

One of the difficulties associated with studying diverse receptor systems such as TCR recognition of pMHC is that it is difficult to extract general rules about the system. However, in the context of what has been done with other TCR-pMHC, there are some general features that we can present from these data. Previous structural studies have highlighted TCR recognition of altered peptide ligands [5; 12], different peptides presented by the same MHC [4; 6; 9; 44], or the effects of mutation in the TCR to binding [45], but not the structural effects of MHC mutation on TCR-pMHC binding. The effects of mutations in the MHC through biological readout, co-crystal structures, and thermodynamics suggest a correlation between T cell response and affinity. As many as 32 hydrogen bonds determine specificity in BM3.3-pBM1/K^b [44], but only 21 in AHIII-p1049/A2 [28] and approximately 15 in the AHIII-p1049/A2(K66A) complex. The recently determined structure of 2C-QL9/L^d [19] reveals an interface with less than 10 hydrogen bonds and entropically favorable binding. What does this say about specificity? If there are no hydrogen bonds determining specificity, the only way the TCR can be sure to only recognize the foreign complex must be complementarity of fit. Not surprisingly perhaps, AHIII-p1049/A2 [28] and 2C-QL9/L^d [19] have the greatest complementarity of fit of all TCR-pMHC structures determined to date. In addition to other published results, our data suggest that the thermodynamics for each TCR-pMHC interaction is unique. The large range of thermodynamic constants reveals that there are many ways to get to T cell activation. This all suggests that the pathways to activation are not important, just the end point.

Most importantly, the AHIII-p1049/A2(K66A) structure provides evidence that a variation in the MHC and not the peptide can directly affect a CDR3 loop. The idea of CDR1 and CDR2 recognition of MHC followed by CDR3 binding to peptide works for a select few TCR, but not for most. In the case of K66, Lys is not conserved across all MHC (93% of HLA-A2 subtypes, but only 42.5% conserved in HLA-A overall, and only 1.5% of HLA-B molecules [34]). Therefore, the presence of this charge is not required, but can be thought of as another piece of the antigen surface. TCR recognition of the pMHC surface cannot be divorced into separate binding events of peptide and MHC.

MATERIALS AND METHODS

Cell Lines and Expression Plasmids

The HLA-A2 mutants transfected into Hmy2.C1R cells have been described previously [23]. All cell lines showed cell surface expression of HLA-A2 at similar levels as wild-type HLA-A2 as detected by the HLA-A2-specific Ab BB7.2 [48].

Protein Production and Purification

Soluble AHIII12.2 TCR was produced as previously described [28]. Briefly, the ectodomains of AHIII TCR α and β chains were expressed as inclusion bodies in *E. coli*. Purified inclusion bodies, previously dissolved in 8M urea, were rapidly injected into a folding buffer optimized for the AHIII TCR at a concentration of 50 μg/ml. After incubation for 36 hours at 10 °C and extensive dialysis the native TCR was purified and concentrated by DE52 anion exchange (Whatman, Florham Park, NJ)) followed by gel filtration chromatography (Phenomenex, Torrance, CA) on HPLC. The purified AHIII TCR was concentrated to 10 mg/ml and stored at -80 °C. Soluble AHIII TCR was tested for proper folding and activity through an ELISA using HLA-A2 tetramer. Typical yield for each 1 L refold is about 3-5 mg of active TCR.

Similarly, soluble HLA-A2 variants were produced as inclusion bodies in *E. coli* and refolded in vitro [49]. Peptide p1049 (ALWGFFPVL), presented by A2, was synthesized by the UNC Peptide Synthesis Facility (Chapel Hill, NC). Briefly, peptide, β_2m, and heavy chain were injected in that order into a folding buffer optimized for refolding class I MHC at a concentration of 50 μg/ml. After incubation for 24-36 hours at 10 °C the folded pMHC was concentrated in an Amicon ultrafiltration cell (Millipore, Billerica, MA) and purified using gel filtration chromatography (Phenomenex) on HPLC. The purified wild-type and A2 variants were concentrated to 10 mg/ml and stored at -80°C. Typical yield for each 1 L refold is about 5 mg of pMHC.

Cytotoxicity Assay

Cytotoxicity was assayed using a standard 4 hour ^{51}Cr release assay as described previously [50]. Briefly, between 5.0×10^3 and 5.0×10^4 AHIII 12.2 T cells were incubated with 5000 peptide-pulsed ^{51}Cr-labeled A2 mutant-transfected cells. Since p1049 is a human self-antigen, the transfectants were recognized without the addition of p1049 to the cells. Additional p1049 did not increase cytotoxicity (data not shown).

Surface Plasmon Resonance Experiments

Five-thousand resonance units (RUs) of H57-597 (capturing molecule, anti-TCR Cβ Ab) were covalently bound to a Biacore CM5 sensor chip (Uppsala, Sweden) using standard amine coupling. Soluble AHIII12.2 TCR (ligand) was then added to the Ab at a concentration of 50-100 nM to generate 300-400 RU of bound TCR. Soluble class I MHC (analyte) was injected onto the surface at a flow rate of 100 μl/min in a 30-s pulse. TCR and MHC were removed from the surface with 0.1 M Glycine, 0.5 M NaCl, pH 2.5, and the procedure was repeated until at least three curves were obtained for the different concentrations of analyte. Curves obtained at each concentration were subtracted from a reference surface that contained Ab alone without TCR or using recombinant P14 TCR as a negative control. Data were processed using Scrubber (BioLogic Software, Campbell, Australia) and CLAMP [51]. The suitability of the fit was measured based on χ^2 values and the appearance of residuals. In all cases, χ^2 was below 1, residuals were small and random, and the experimental curves visually matched the predicted curves.

Protein Crystallization and Structure Determination

The crystallization conditions for the co-crystal complexes were similar to those optimized for AHIII TCR with wild-type A2 [28]. Briefly, crystals are grown by hanging drop, vapor diffusion, using AHIII TCR and A2 variants mixed at equal ratios at a concentration of 10 mg/ml. Drops contain 1 μl of protein mixed with 1 μl of a well solution containing Hepes, pH 7.5-8.0, 1 M NaCl, and 14%-18% PEG 8000. Small crystals formed within 3 days along with precipitate in drops. Crystal size was improved by macro-seeding into identical conditions. Crystals were transferred to mother liquor containing 25% glycerol as cryoprotectant. Crystallographic data were collected at Southeast Regional Collaborative Access Team (SER-CAT) 22-ID and 22-BM beamlines at the Advanced Photon Source, Argonne National Laboratory (Argonne, IL). Data for AHIII-p1049/A2(T163A) was collected on the 22-BM beamline at 12,398.42 eV for 360° at a distance of 200 mm using 1.0° oscillations. Two datasets for AHIII-p1049/A2 (W167A) were collected on the 22-ID beamline at 12,759.89 eV at a distance of 300 mm using 1.0° oscillations. 180° were collected at an omega angle of 90° and an additional 45° was collected at an omega of 45°. These data sets were indexed separately and then scaled together. Data for AHIII-p1049/A2(K66A) was collected on the 22-ID beamline at 12,759.89 eV for 180° at a distance of 300 mm using 1.0° oscillations. Data for all co-crystal complexes were indexed and scaled with HKL2000 [52]. The data for AHIII-p1049/A2(T163A) was originally collected out to 2.1 Å, but it was highly anisotropic. As a result, the statistics in the highest shells were poor, so the data was truncate at 2.4 Å. Molecular replacement solutions were determined using Rigid Body Refinement in Refmac 5.0 [53] with AHIII-p1049/A2 (1LP9) [28] as the search model. Temperature factors were set to 30.0 using Moleman [54]. Positional refinement using noncrystallographic symmetry restraints for the first few cycles and TLS refinement [55] in Refmac 5.0 was performed iteratively with manual intervention with O [56]. When the statistics did not improve over two subsequent rounds of refinement and the Rfree was below 30%, waters were added using Arp within Refmac 5.0 to AHIII-p1049/A2(T163A) and AHIII-p1049/A2(W167A) models. All waters were examined to confirm the presence of hydrogen bond donors or acceptors at reasonable geometries. For the AHIII-p1049/A2(K66A) model, an omit map of the CDR3α loop was generated to verify the conformational change. The refinement statistics for the final models are presented in Table 2. Surface complementarity (SC) calculated using Sc [57] in CCP4 [53].

Isothermal Titration Calorimetry

ITC experiments on AHIII TCR with wild-type p1049/A2 and p1049/A2(K66A) were performed on a Microcal VP-ITC in the UNC Macromolecular Interactions Facility (Chapel Hill, NC). Thermodynamic constants were obtained for AHIII TCR binding wild-type p1049/A2 as well as p1049/A2(K66A) by fitting the calorimetric data using a one-site binding model in Microcal Origin Version 5.0 Software (OriginLab Corporation, Northampton, MA). Soluble AHIII TCR was placed in the mixing chamber. p1049/A2 or p1049/A2(K66A) was titrated into the AHIII TCR solution until binding reached saturation. Titration of wild-type p1049/A2 into AHIII TCR was performed in duplicate, once in Phosphate buffer, pH 7.5, and then in Tris buffer, pH 7.5, to ensure that the determined enthalpy was not affected by ionization enthalpy of the buffer [58]. Concentrations of AHIII TCR and p1049/A2 were 17 μM and 217 μM, respectively, in Phosphate and 19 μM and 234 μM, respectively in Tris. For wild-type p1049/A2 experiments, a volume of 3 μL was used for the first four injections, and then 5 μL for the remaining titrations. The baseline, generated by averaging the heat measured for the last 10 injections, was subtracted from all peaks. Titration of p1049/A2(K66A) in AHIII TCR was performed in triplicate in Phosphate buffer, pH 7.5. Concentrations of AHIII TCR and p1049/A2(K66A) were 40 μM and 618 μM, 65 μM and 450 μM, and 43 μM and 394 μM, respectively, for the three replicates. For all p1049/A2(K66A) experiments, 5 μL was injected for the first four peaks, increasing to 10 μL for the remainder of the experiment. Because of the relatively small amount of heat released upon AHIII-p1049/A2(K66A) binding, a more accurate baseline

was determined by injecting p1049/A2(K66A) into Phosphate buffer to measure heat of dilution. This reference data set was then subtracted from the experimental data set in Origin Software. All concentrations were determined before the proteins were placed in the microcalorimeter using extinction coefficients. ΔH and ΔS were calculated using the Origin software. Gibbs free energy was calculated as $\Delta G = \Delta H - T\Delta S$, T = 298 K.

ACKNOWLEDGEMENTS

We thank William E. Biddison, Ph.D. of the Molecular Immunology Section of the National Institutes of Health, Bethesda, MD for supplying the HLA-A2 variant cells lines for our cytotoxicity assays. Data were collected at Southeast Regional Collaborative Access Team (SER-CAT) 22-ID beamline at the Advanced Photon Source, Argonne National Laboratory. Staff at the beamline are acknowledged for assistance in data collection. Use of the Advanced Photon Source was supported by the U. S. Department of Energy, Office of Science, Office of Basic Energy Sciences, under Contract No. W-31-109-Eng-38. The director of the UNC Macromolecular Interations Facility, Ashutosh Tripathy, Ph.D. is gratefully acknowledged for his assistance with collecting and interpreting ITC data. Members of the Collins and Frelinger labs are acknowledged for helpful discussions.

References

1. Schatz DG, Spanopoulou E. Biochemistry of V(D)J recombination. Curr Top Microbiol Immunol 2005;290:49–85. [PubMed: 16480039]
2. Spicuglia S, Franchini DM, Ferrier P. Regulation of V(D)J recombination. Curr Opin Immunol 2006;18:158–63. [PubMed: 16459067]
3. Rudolph MG, Stanfield RL, Wilson IA. How TCRs bind MHCs, peptides, and coreceptors. Annu Rev Immunol 2006;24:419–66. [PubMed: 16551255]
4. Degano M, Garcia KC, Apostolopoulos V, Rudolph MG, Teyton L, Wilson IA. A functional hot spot for antigen recognition in a superagonist TCR/MHC complex. Immunity 2000;12:251–61. [PubMed: 10755612]
5. Ding YH, Baker BM, Garboczi DN, Biddison WE, Wiley DC. Four A6-TCR/peptide/HLA-A2 structures that generate very different T cell signals are nearly identical. Immunity 1999;11:45–56. [PubMed: 10435578]
6. Garcia KC, Degano M, Pease LR, Huang M, Peterson PA, Teyton L, Wilson IA. Structural basis of plasticity in T cell receptor recognition of a self peptide-MHC antigen. Science 1998;279:1166–72. [PubMed: 9469799]
7. Reiser JB, Gregoire C, Darnault C, Mosser T, Guimezanes A, Schmitt-Verhulst AM, Fontecilla-Camps JC, Mazza G, Malissen B, Housset D. A T cell receptor CDR3beta loop undergoes conformational changes of unprecedented magnitude upon binding to a peptide/MHC class I complex. Immunity 2002;16:345–54. [PubMed: 11911820]
8. Kjer-Nielsen L, Clements CS, Purcell AW, Brooks AG, Whisstock JC, Burrows SR, McCluskey J, Rossjohn J. A structural basis for the selection of dominant alphabeta T cell receptors in antiviral immunity. Immunity 2003;18:53–64. [PubMed: 12530975]
9. Reiser JB, Darnault C, Gregoire C, Mosser T, Mazza G, Kearney A, van der Merwe PA, Fontecilla-Camps JC, Housset D, Malissen B. CDR3 loop flexibility contributes to the degeneracy of TCR recognition. Nat Immunol 2003;4:241–7. [PubMed: 12563259]
10. Garboczi DN, Ghosh P, Utz U, Fan QR, Biddison WE, Wiley DC. Structure of the complex between human T-cell receptor, viral peptide and HLA-A2. Nature 1996;384:134–41. [PubMed: 8906788]
11. Tynan FE, Reid HH, Kjer-Nielsen L, Miles JJ, Wilce MC, Kostenko L, Borg NA, Williamson NA, Beddoe T, Purcell AW, Burrows SR, McCluskey J, Rossjohn J. A T cell receptor flattens a bulged antigenic peptide presented by a major histocompatibility complex class I molecule. Nat Immunol 2007;8:268–76. [PubMed: 17259989]
12. Chen JL, Stewart-Jones G, Bossi G, Lissin NM, Wooldridge L, Choi EM, Held G, Dunbar PR, Esnouf RM, Sami M, Boulter JM, Rizkallah P, Renner C, Sewell A, van der Merwe PA, Jakobsen BK, Griffiths G, Jones EY, Cerundolo V. Structural and kinetic basis for heightened immunogenicity of T cell vaccines. J Exp Med 2005;201:1243–55. [PubMed: 15837811]

13. Lee JK, Stewart-Jones G, Dong T, Harlos K, Di Gleria K, Dorrell L, Douek DC, van der Merwe PA, Jones EY, McMichael AJ. T cell cross-reactivity and conformational changes during TCR engagement. J Exp Med 2004;200:1455–66. [PubMed: 15583017]

14. Krogsgaard M, Prado N, Adams EJ, He XL, Chow DC, Wilson DB, Garcia KC, Davis MM. Evidence that structural rearrangements and/or flexibility during TCR binding can contribute to T cell activation. Mol Cell 2003;12:1367–78. [PubMed: 14690592]

15. Willcox BE, Gao GF, Wyer JR, Ladbury JE, Bell JI, Jakobsen BK, van der Merwe PA. TCR binding to peptide-MHC stabilizes a flexible recognition interface. Immunity 1999;10:357–65. [PubMed: 10204491]

16. Garcia KC, Radu CG, Ho J, Ober RJ, Ward ES. Kinetics and thermodynamics of T cell receptor-autoantigen interactions in murine experimental autoimmune encephalomyelitis. Proc Natl Acad Sci U S A 2001;98:6818–23. [PubMed: 11391002]

17. Ely LK, Beddoe T, Clements CS, Matthews JM, Purcell AW, Kjer-Nielsen L, McCluskey J, Rossjohn J. Disparate thermodynamics governing T cell receptor-MHC-I interactions implicate extrinsic factors in guiding MHC restriction. Proc Natl Acad Sci U S A 2006;103:6641–6. [PubMed: 16617112]

18. Davis-Harrison RL, Armstrong KM, Baker BM. Two different T cell receptors use different thermodynamic strategies to recognize the same peptide/MHC ligand. J Mol Biol 2005;346:533–50. [PubMed: 15670602]

19. Colf LA, Bankovich AJ, Hanick NA, Bowerman NA, Jones LL, Kranz DM, Garcia KC. How a single T cell receptor recognizes both self and foreign MHC. Cell 2007;129:135–46. [PubMed: 17418792]

20. Ellis JM, Henson V, Slack R, Ng J, Hartzman RJ, Katovich Hurley C. Frequencies of HLA-A2 alleles in five U.S. population groups. Predominance Of A*02011 and identification of HLA-A*0231. Hum Immunol 2000;61:334–40. [PubMed: 10689125]

21. Baker BM, Turner RV, Gagnon SJ, Wiley DC, Biddison WE. Identification of a crucial energetic footprint on the alpha1 helix of human histocompatibility leukocyte antigen (HLA)-A2 that provides functional interactions for recognition by tax peptide/HLA-A2-specific T cell receptors. J Exp Med 2001;193:551–62. [PubMed: 11238586]

22. Baxter TK, Gagnon SJ, Davis-Harrison RL, Beck JC, Binz AK, Turner RV, Biddison WE, Baker BM. Strategic mutations in the class I major histocompatibility complex HLA-A2 independently affect both peptide binding and T cell receptor recognition. J Biol Chem 2004;279:29175–84. [PubMed: 15131131]

23. Wang Z, Turner R, Baker BM, Biddison WE. MHC allele-specific molecular features determine peptide/HLA-A2 conformations that are recognized by HLA-A2-restricted T cell receptors. J Immunol 2002;169:3146–54. [PubMed: 12218132]

24. Gagnon SJ, Borbulevych OY, Davis-Harrison RL, Baxter TK, Clemens JR, Armstrong KM, Turner RV, Damirjian M, Biddison WE, Baker BM. Unraveling a hotspot for TCR recognition on HLA-A2: evidence against the existence of peptide-independent TCR binding determinants. J Mol Biol 2005;353:556–73. [PubMed: 16197958]

25. Engelhard VH, Benjamin C. Isolation and characterization of monoclonal mouse cytotoxic T lymphocytes with specificity for HLA-A,B or -DR alloantigens. J Immunol 1982;129:2621–9. [PubMed: 6982933]

26. Henderson RA, Cox AL, Sakaguchi K, Appella E, Shabanowitz J, Hunt DF, Engelhard VH. Direct identification of an endogenous peptide recognized by multiple HLA-A2.1-specific cytotoxic T cells. Proc Natl Acad Sci U S A 1993;90:10275–9. [PubMed: 7694286]

27. Buslepp J, Kerry SE, Loftus D, Frelinger JA, Appella E, Collins EJ. High affinity xenoreactive TCR:MHC interaction recruits CD8 in absence of binding to MHC. J Immunol 2003;170:373–83. [PubMed: 12496422]

28. Buslepp J, Wang H, Biddison WE, Appella E, Collins EJ. A correlation between TCR Valpha docking on MHC and CD8 dependence: implications for T cell selection. Immunity 2003;19:595–606. [PubMed: 14563323]

29. Tynan FE, Burrows SR, Buckle AM, Clements CS, Borg NA, Miles JJ, Beddoe T, Whisstock JC, Wilce MC, Silins SL, Burrows JM, Kjer-Nielsen L, Kostenko L, Purcell AW, McCluskey J, Rossjohn

J. T cell receptor recognition of a 'super-bulged' major histocompatibility complex class I-bound peptide. Nat Immunol 2005;6:1114–22. [PubMed: 16186824]

30. Clements CS, Dunstone MA, Macdonald WA, McCluskey J, Rossjohn J. Specificity on a knife-edge: the alphabeta T cell receptor. Curr Opin Struct Biol 2006;16:787–95. [PubMed: 17011774]
31. Delano, WL. The PyMOL Molecular Graphics System. DeLano Scientific; San Carlos, CA: 2002.
32. Lovell SC, Davis IW, Arendall WB 3rd, de Bakker PI, Word JM, Prisant MG, Richardson JS, Richardson DC. Structure validation by Calpha geometry: phi,psi and Cbeta deviation. Proteins 2003;50:437–50. [PubMed: 12557186]
33. Madden DR. The three-dimensional structure of peptide-MHC complexes. Annu Rev Immunol 1995;13:587–622. [PubMed: 7612235]
34. Robinson J, Waller MJ, Parham P, de Groot N, Bontrop R, Kennedy LJ, Stoehr P, Marsh SG. IMGT/HLA and IMGT/MHC: sequence databases for the study of the major histocompatibility complex. Nucleic Acids Res 2003;31:311–4. [PubMed: 12520010]
35. Ding YH, Smith KJ, Garboczi DN, Utz U, Biddison WE, Wiley DC. Two human T cell receptors bind in a similar diagonal mode to the HLA-A2/Tax peptide complex using different TCR amino acids. Immunity 1998;8:403–11. [PubMed: 9586631]
36. Davis-Harrison RL, Insaidoo FK, Baker BM. T Cell Receptor Binding Transition States and Recognition of Peptide/MHC. Biochemistry 2007;46:1840–50. [PubMed: 17249694]
37. Wu W, Harley PH, Punt JA, Sharrow SO, Kearse KP. Identification of CD8 as a peanut agglutinin (PNA) receptor molecule on immature thymocytes. J Exp Med 1996;184:759–64. [PubMed: 8760831]
38. Wu LC, Tuot DS, Lyons DS, Garcia KC, Davis MM. Two-step binding mechanism for T-cell receptor recognition of peptide MHC. Nature 2002;418:552–6. [PubMed: 12152083]
39. James LC, Roversi P, Tawfik DS. Antibody multispecificity mediated by conformational diversity. Science 2003;299:1362–7. [PubMed: 12610298]
40. Chothia C, Lesk AM, Tramontano A, Levitt M, Smith-Gill SJ, Air G, Sheriff S, Padlan EA, Davies D, Tulip WR, et al. Conformations of immunoglobulin hypervariable regions. Nature 1989;342:877–83. [PubMed: 2687698]
41. Chothia C, Lesk AM, Gherardi E, Tomlinson IM, Walter G, Marks JD, Llewelyn MB, Winter G. Structural repertoire of the human VH segments. J Mol Biol 1992;227:799–817. [PubMed: 1404389]
42. Al-Lazikani B, Lesk AM, Chothia C. Standard conformations for the canonical structures of immunoglobulins. J Mol Biol 1997;273:927–48. [PubMed: 9367782]
43. Morea V, Tramontano A, Rustici M, Chothia C, Lesk AM. Conformations of the third hypervariable region in the VH domain of immunoglobulins. J Mol Biol 1998;275:269–94. [PubMed: 9466909]
44. Reiser JB, Darnault C, Guimezanes A, Gregoire C, Mosser T, Schmitt-Verhulst AM, Fontecilla-Camps JC, Malissen B, Housset D, Mazza G. Crystal structure of a T cell receptor bound to an allogeneic MHC molecule. Nat Immunol 2000;1:291–7. [PubMed: 11017099]
45. Borg NA, Ely LK, Beddoe T, Macdonald WA, Reid HH, Clements CS, Purcell AW, Kjer-Nielsen L, Miles JJ, Burrows SR, McCluskey J, Rossjohn J. The CDR3 regions of an immunodominant T cell receptor dictate the 'energetic landscape' of peptide-MHC recognition. Nat Immunol 2005;6:171–80. [PubMed: 15640805]
46. Murshudov GN, Vagin AA, Dodson EJ. Refinement of macromolecular structures by the maximum-likelihood method. Acta Crystallogr D Biol Crystallogr 1997;53:240–55. [PubMed: 15299926]
47. Reed, N. S. P. a. R. J. Improved Structure Refinement Through Maximum Likelihood. Acta Crystallogr A 1996;52:659–668.
48. Brodsky FM, Parham P, Barnstable CJ, Crumpton MJ, Bodmer WF. Monoclonal antibodies for analysis of the HLA system. Immunol Rev 1979;47:3–61. [PubMed: 95015]
49. Garboczi DN, Hung DT, Wiley DC. HLA-A2-peptide complexes: refolding and crystallization of molecules expressed in Escherichia coli and complexed with single antigenic peptides. Proc Natl Acad Sci U S A 1992;89:3429–33. [PubMed: 1565634]
50. Loftus DJ, Chen Y, Covell DG, Engelhard VH, Appella E. Differential contact of disparate class I/peptide complexes as the basis for epitope cross-recognition by a single T cell receptor. J Immunol 1997;158:3651–8. [PubMed: 9103427]

51. Myszka DG, Morton TA. CLAMP: a biosensor kinetic data analysis program. Trends Biochem Sci 1998;23:149–50. [PubMed: 9584619]

52. Otwinowski, Z. a. M., M. CarterCWJ. a. R. M. S.Macromolecular Crystallography, part A edit. Methods in Enzymology. Processing of X-ray Diffraction Data Collected in Oscillation Mode1997276Academic PressNew York

53. The CCP4 suite: programs for protein crystallography. Acta Crystallogr D Biol Crystallogr 1994;50:760–3. [PubMed: 15299374]

54. Kleywegt, GJ. Uppsala University; Uppsala, Sweden: 19922004.

55. Winn MD, Isupov MN, Murshudov GN. Use of TLS parameters to model anisotropic displacements in macromolecular refinement. Acta Crystallogr D Biol Crystallogr 2001;57:122–33. [PubMed: 11134934]

56. Jones TA, Zou JY, Cowan SW, Kjeldgaard. Improved methods for building protein models in electron density maps and the location of errors in these models. Acta Crystallogr A 1991;47(Pt 2):110–9. [PubMed: 2025413]

57. Lawrence MC, Colman PM. Shape complementarity at protein/protein interfaces. J Mol Biol 1993;234:946–50. [PubMed: 8263940]

58. Baker BM, Murphy KP. Evaluation of linked protonation effects in protein binding reactions using isothermal titration calorimetry. Biophys J 1996;71:2049–55. [PubMed: 8889179]

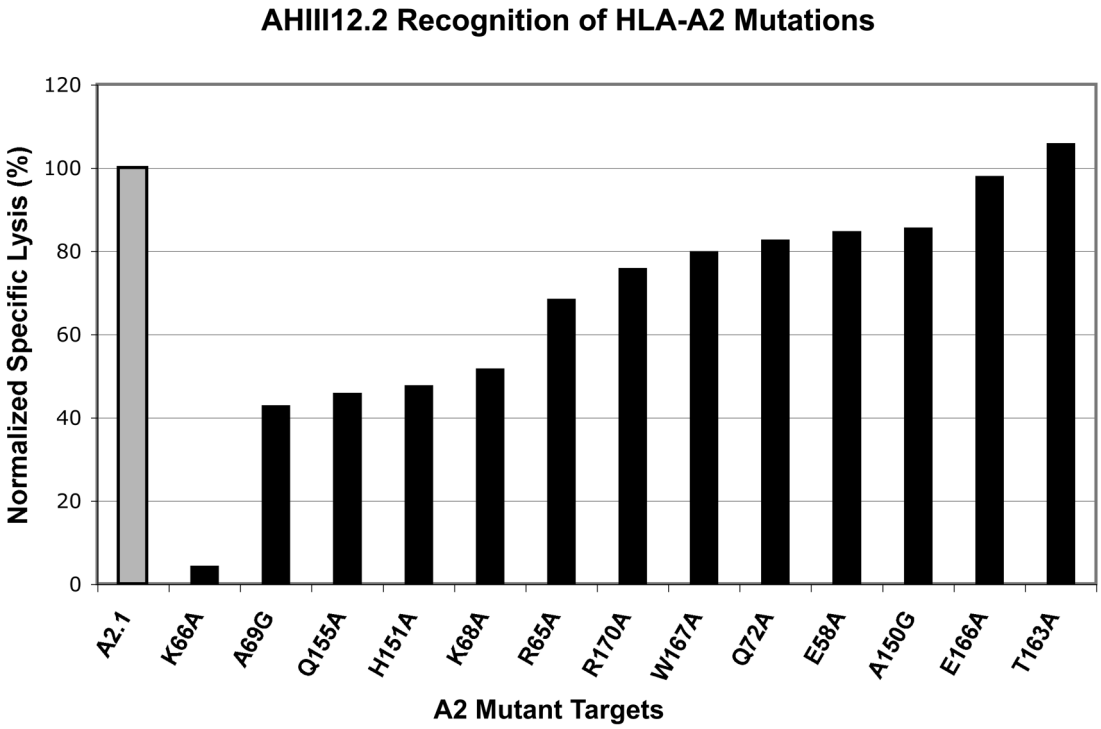

Figure 1. CTL Killing as a Function of Substitutions in the p1049/A2 Complex

Cytotoxic lysis assays (^{51}Cr release assays) were performed with AHIII T cells against cells expressing mutant A2 complexes. Data was normalized such that lytic activity against native HLA-A2 is 100%.

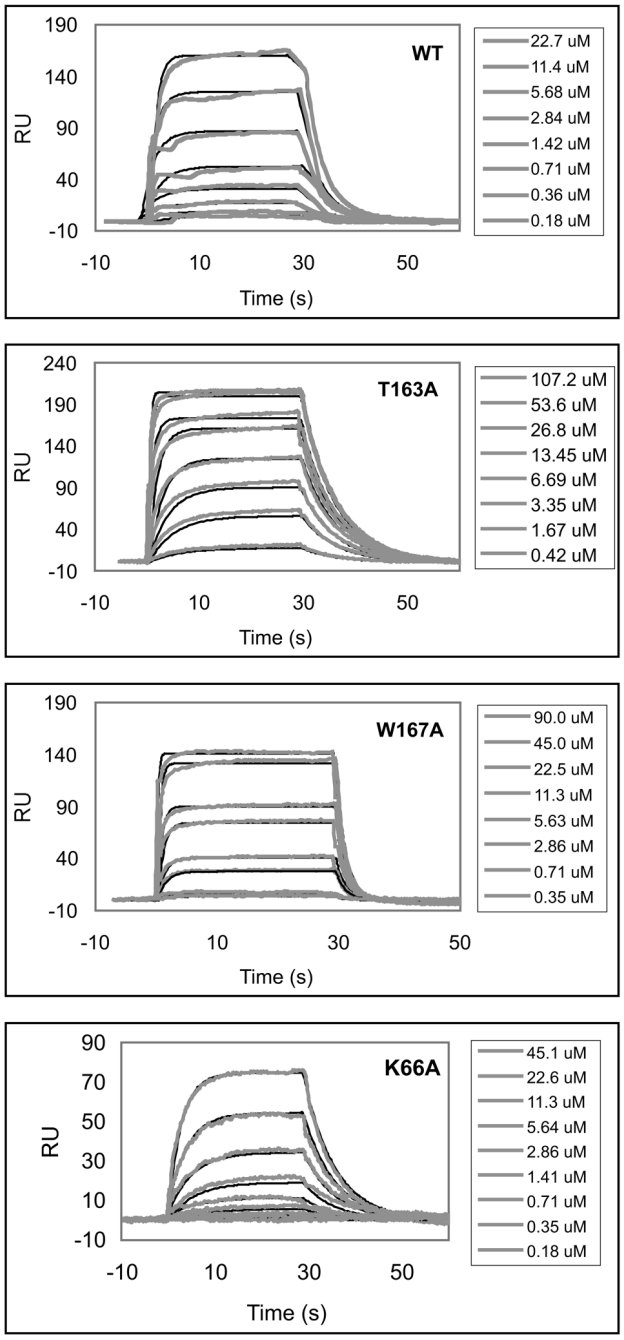

Figure 2. AHIII TCR binding to p1049/A2 variants as measured by SPR

Kinetic data between AHIII TCR and wild-type p1049/A2 as well as p1049/A2 mutants at various pMHC concentrations were obtained using SPR and globally fit to a reversible bimolecular reaction using Clamp [51]. Model binding curves are drawn in black. Curve fits are drawn in grey.

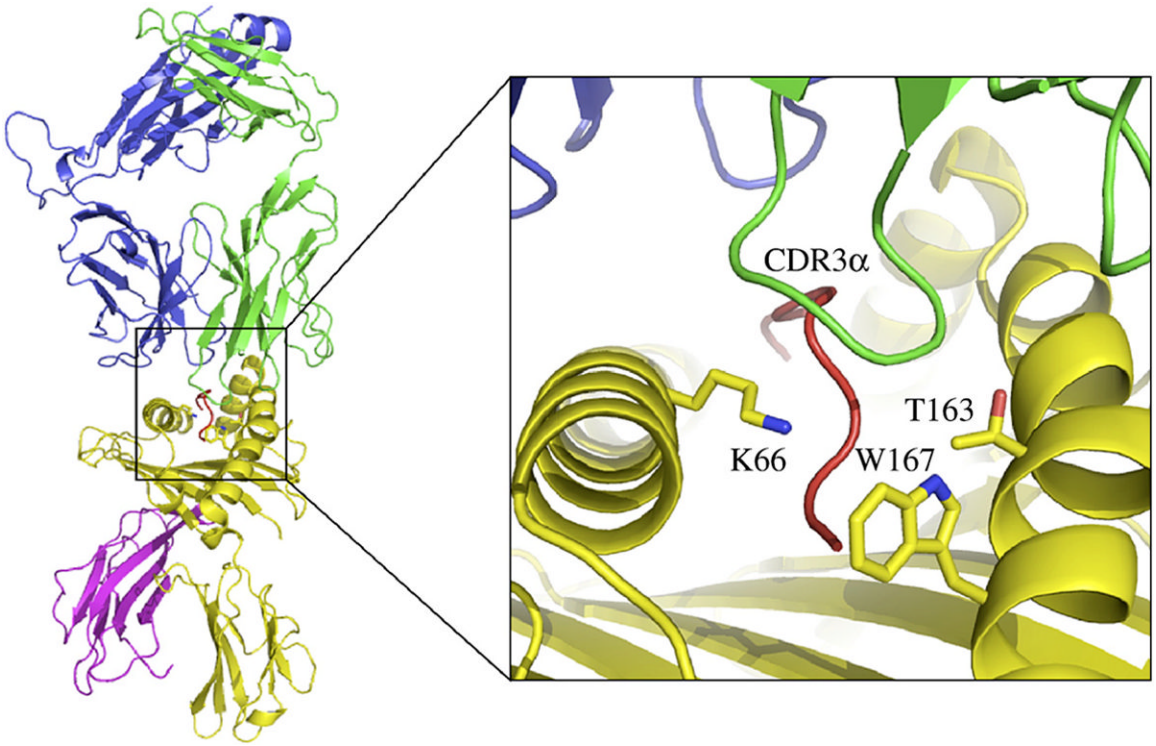

Figure 3. Structure of AHIII TCR bound to p1049/A2

The AHIII TCR alpha (green) and beta (blue) chains, interact with the p1049/A2 surface via CDR loops. HLA-A2, consisting of a heavy chain (yellow) and β_2m (magenta), present the peptide, p1049 (red). (Inset) The surface of the p1049/A2 is contacted by the CDR loops of the AHIII TCR. Residues that have been mutated to alanine for structural experiments (T163, W167, K66) are shown. Figure generated using PDB coordinates 1LP9 and PyMol [31].

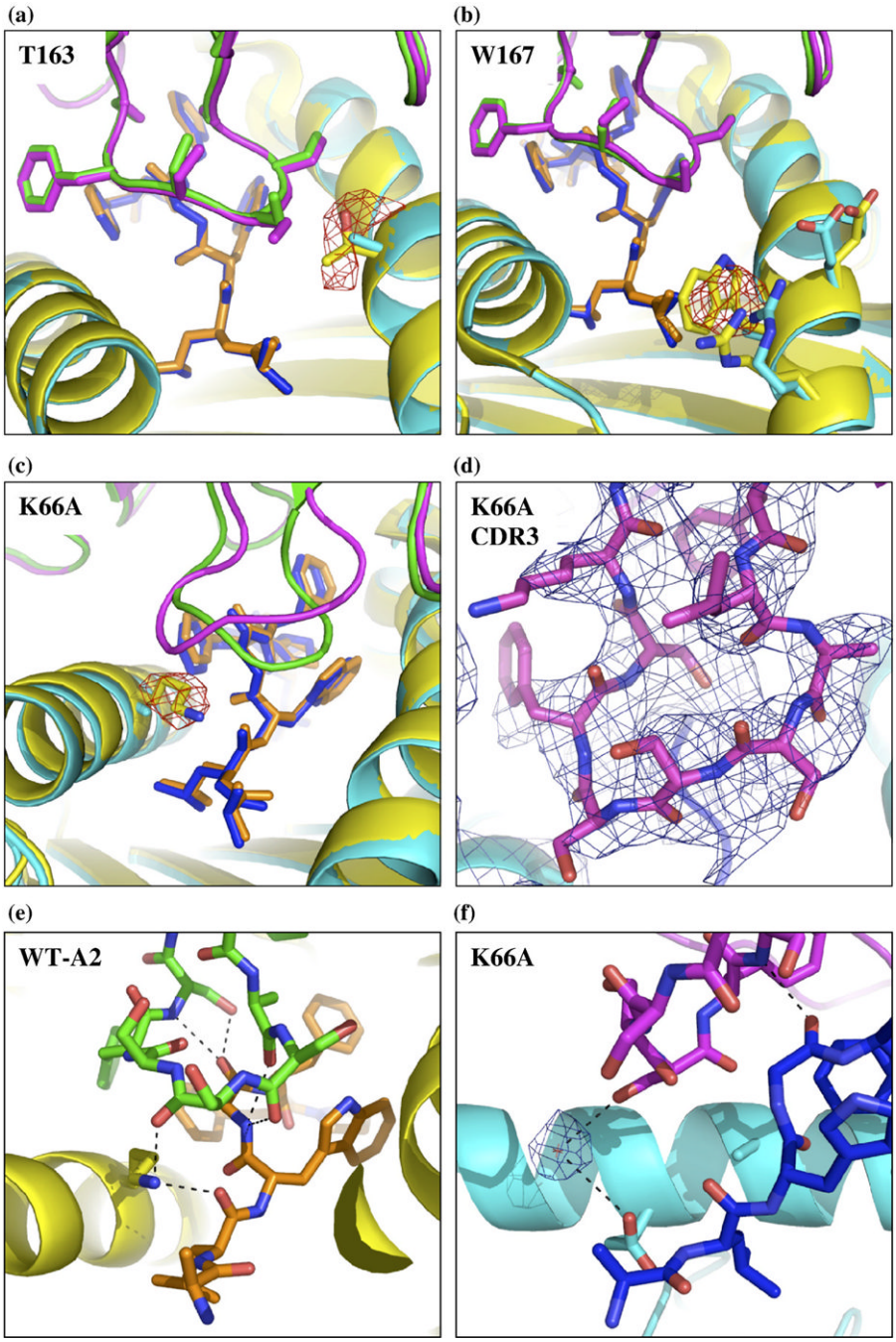

Figure 4. Mutation of Lys66 to alanine results in large change in CDR3α loop

(a) Complex of AHIII TCR bound to p1049/A2(T163A) superimposed onto wild-type structure of AHIII-A2. Mutant A2 (cyan) and peptide (blue) show little difference from wild-type A2 (yellow) and peptide (orange). Conformations of TCR CDR2 and CDR3 loops and side chains are no different between mutant (magenta) and wild-type (green) structures (coloring scheme same for all panels). (b) Complex of AHIII TCR bound to p1049/A2(W167A) also shows no change in TCR structure and only minor alterations in local MHC side chains. (c) Superimposition with of AHIII TCR bound to p1049/A2(K66A) onto wild-type shows a major rearrangement of the AHIII CDR3α loop, while the structure of pMHC remains unchanged. (a, b, c) Mutations at T163A, W167A, and K66A are confirmed by difference electron density

($Fobs_{wild\text{-}type}$ - $Fobs_{mutant}$) contoured at -3σ surrounding the side chains. (d) 2Fobs-Fcalc density map (blue), contoured at 1 σ, confirms placement of final modeled CDR3α loop at 2.88 Å. (e) Five hydrogen bond interactions occur between AHIII TCR CDR3α and wild-type p1049/A2. As shown above some or all of these bonds may be broken due to loop movement. (f) The 2Fobs-Fcalc electron density suggests the presence of a water molecule in the AHIII-p1049/A2(K66A) structure, which would allow for a water-mediated hydrogen bond between Glu63 of A2 and Ser100 on CDR3α of AHIII (water shown for illustration, but not included in PDB). The only other possible hydrogen bond to CDR3α is from the Ser102 nitrogen to the Gly4 oxygen of the peptide. Figures generated using PyMol [31].

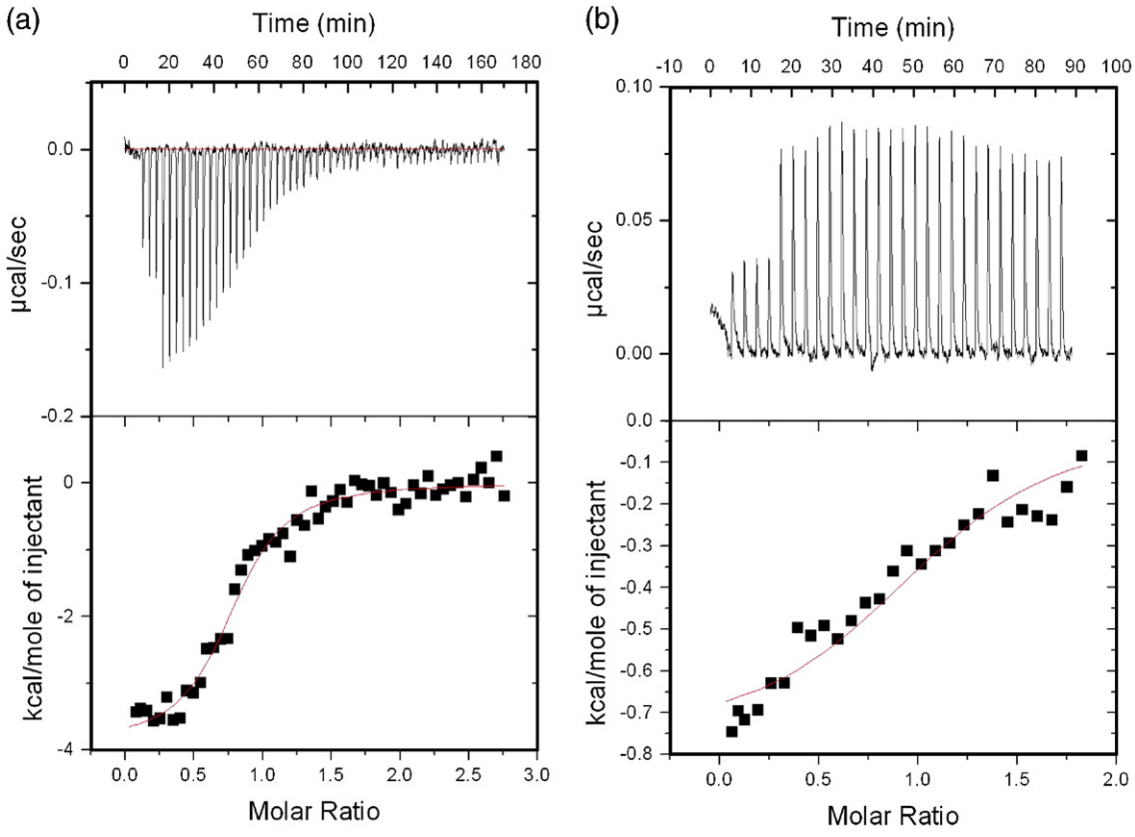

Figure 5. K66A mutation in p1049/A2 dramatically decreases the enthalpy of binding

The binding enthalpy of AHIII TCR was measured directly with ITC for both wild-type p1049/A2, and p1049/A2(K66A). (a) Power versus molar ratio plot for titration of 234 μM p1049/A2 into 19 μM of AHIII TCR (upper panel) and plot of integrated heat versus molar ratio after baseline correction (lower panel). The baseline was generated by averaging heat measured for last 10 injections. (b) Plot of power versus molar ratio for titration of 394 μM p1049/A2(K66A) into 40 μM of AHIII TCR (upper panel) and integrated heat versus molar ratio after baseline correction (lower panel). The baseline derived from titrating p1049/A2(K66A) into buffer alone. All experiments performed at 25 °C. The fitted curves are from the model for single-site binding provided in Microcal Origin Software. Thermodynamic parameters determined are presented in Table 4.

Table 1

Equilibrium and kinetic binding parameters for AHIII TCR binding p1049/A2 mutants.

pMHC Complex	K_d Equilibrium (μM)	K_d Kinetic (μM)	k_{on} ($\times 10^4$ $M^{-1}s^{-1}$)	k_{off} (s^{-1})
p1049/A2	9.3	8.7	3.1	0.27
p1049/A2(T163A)	4.7	4.6	3.3	0.16
p1049/A2(W167A)	15.4	14.8	4.1	0.63
p1049/A2(K66A)	31.8	34.0	0.47	0.15

Parameters were obtained by fitting data with Scrubber 2.0 and CLAMP. Kinetic dissociation constants (K_d) were obtained from kinetic data using the determined k_{on} and k_{off} values. Equilibrium dissociation constants were obtained separately by fitting maximum binding responses for various concentrations of pMHC using Scrubber.

Table 2

Data Statistics

	AHIII-p1049/A2(T163A)	AHIII-p1049/A2(W167A)	AHIII-p1049/A2(K66A)
Data Collection			
Space Group	$P2_1$	$P2_1$	$P2_1$
Cell Dimensions	a=93.49 Å, b=84.18 Å, c=121.77 Å, β=92.05°	a=94.28 Å, b=84.35 Å, c=122.47 Å, β=92.53°	a=93.42 Å, b=83.89 Å, c=122.27 Å, β=92.21°
Molecules/AU	2	2	2
Resolution	50.0 - 2.10 Å	50.0 - 2.5 Å	50.0 - 2.88 Å
R_{merge}(%)[a,b]	5.9 (46.7)	6.6 (31.8)	7.8 (42.1)
<I/σ>[c]	11.4 (1.6)	18.0 (1.8)	11.2 (1.3)
Unique Reflections	76,682	61,781	40,707
Avg. Redundancy	2.7 (1.7)	4 (2.5)	3.4 (2.3)
Completeness (%)	70.0 (24.7)	92.8 (67.8)	95.7 (69.0)
Solvent Content (%)	41.5	40.7	44.1
Refinement			
Resolution Range	30.0 - 2.4 Å	30.0 - 2.5 Å	30.0 - 2.88 Å
Number of Reflections	59,694	58,660	38,683
R_{fac}[d]	24.0	25.3	26.8
R_{free}	28.9	29.9	29.3
Number of non-H atoms	13,160	12,995	12,956
Number of waters modeled	267	52	0
<Rs fit>[e]	93%	93%	90%
Coordinate error[f], 46; 47	0.25	0.32	0.46
Deviations from ideality			
Bond lengths	0.006 Å	0.006 Å	0.005 Å
Bond angles	1.040°	1.192°	0.750°
<Temperature Factor>			
Overall	37.6	49.7	47.2
TCR	37.8	49.6	47.5
MHC	37.6	50.1	47.1
Peptide	34.7	48.6	37.5
Ramachandran			
Most favored	1305 (91.4%)	1291 (90.7%)	1287 (90.4%)
Additional allowed	121 (8.5%)	131 (9.2%)	134 (9.4%)
Generously allowed	0	0	0
Disallowed	2 (0.1%)	2 (0.1%)	2 (0.1%)
PDB Entry	2UWE	2JCC	2J8U

[a] $R_{merge} = \Sigma_{hkl}\Sigma_i | I_i - \langle I \rangle | \ / \ \Sigma_{hkl}\Sigma_i I_i$, where I_i is the observed intensity and ⟨I⟩ is the average intensity of multiple observations of symmetry related reflections.

[b] Number in parentheses refers to highest resolution shell.

[c] I/sigI for highest shells : 2.49 - 2.37 Å, 2.59 - 2.50 Å, 3.0 - 2.9 Å (T163A, W167A, and K66A, respectively).

[d] $R = \Sigma_{hkl} | \ | F_{obs} | - k | F_{cal} | \ | \ / \ \Sigma_{hkl} | F_{obs} |$, where R_{free} is calculated for a randomly chosen 5% of reflections, R_{work} is calculated for the remaining 95% of reflections used for structure refinement.

[e] ⟨Rs fit⟩ is the average real space fit of all atoms on a 2fo- fc electron density map.

[f] Error is the mean coordinate error estimate based on maximum likelihood measurements.

Table 3

CDR3α Movement

Residue	Distance (Å)
Leu96	1.0
Ala97	4.2
Ser98	2.6
Ser99	3.0
Ser100	2.6
Phe101	0.3
Ser102	1.7
Lys103	0.7
Mean	2.0

Distances limited to 2 significant figures due to low resolution of AHIII-p1049/A2(K66A).

Table 4

Thermodynamic Parameters of TCR-pMHC Binding as Measured by ITC

Complex	ΔH (kcal/mol)	TΔS (kcal/mol)	ΔG (kcal/mol)	K_d (μM)	Reference
AHIII-p1049/A2	-3.9[a]	4.4	-8.3	1 ± 5	
AHIII-p1049/A2(K66A)	-0.6[b]	6.3	-6.9	7 ± 20	
A6-Tax/A2	5.7	13.6	-7.9	2.2	18
JM22-flu/A2	-19.7	-12.6[c]	-7.1[c]	6.6[c]	15
2C-dEV8/K[b]	-22.7	-16.2	-6.3	84	17
2C-QL9/L[d]	-4.19	3.4	-7.6	2	19
LC13-FLR/B8	-3.6	3.4	-7.0	8.1 ± 2.7	17
2B4-MCC/IE[k]	-14.8	-8.2	-6.7	12.6 ± 7	14
2B4-K5/IE[k]	-13.5	-6.4	-7.2	6.2 ± 0.2	14

[a] error < 5%

[b] error < 20%

[c] van't Hoff calculation